Monthly Notices of the ROYAL ASTRONOMICAL SOCIETY

MNRAS **551,** 1–5 (2026)
https://doi.org/10.1093/mnras/stag1613
Advance Access publication 2026 August 26
Letter

Concerns regarding recurrent fluorescence's impact on smaller diffuse ISM aromatics

Daniel Majaess [1]★ Cercis Morera-Boado,[2] Tina A. Harriott[3] and Chérif F. Matta [1]

[1]*Department of Chemistry and Physics, Mount Saint Vincent University, Halifax, Nova Scotia B3M2J6, Canada*
[2]*IXM- Secihti-Centro de Investigaciones Químicas, IICBA, Universidad Autónoma del Estado de Morelos, Cuernavaca 62209, Morelos, Mexico*
[3]*Department of Mathematics and Statistics, Mount Saint Vincent University, Halifax, Nova Scotia B3M2J6, Canada*

Accepted 2026 August 18. Received 2026 August 17; in original form 2026 July 19

ABSTRACT

Recent research implied that recurrent fluorescence (RF) could bolster smaller aromatics against fragmentation in the diffuse ISM, yet that hypothesis is contested by time-scales for unrelenting dissociative recombination (electrons), and unceasing dissociating photons. Specifically, neutral cyanonaphthalene can sustain 13.6 eV photoionization, and the ensuing cation's excess energy is channeled through intramolecular vibrational redistribution (IVR), with RF providing the radiative stabilization pathway ($\simeq$ 7 eV negligible survival limit). However, that cation endures dissociative recombination every $\tau \approx 0.5^{+5.6}_{-0.4}$ yr, which deposits $\simeq$ 8.6 eV and exceeds the limit. Moreover, that is paired with 7–13.6 eV photodestruction each $\tau \approx 16^{+223}_{-14}$ yr (total visual dust extinction $A_V = 0$–1, and $\tau \approx 4^{+7}_{-2}$ yr for $A_V \approx 0$). Recent laboratory characterizations of RF were seminal, but the mechanism may not overturn models indicating a gap in smaller $N_C \approx 7$–11 diffuse ISM aromatics, nor support those molecules as viable diffuse interstellar band carriers.

Key words: ISM: molecules.

1 INTRODUCTION

Recent research highlighted or reiterated that the prior consensus on the dissociation of smaller aromatics in harsh environments is debatable (e.g. the diffuse ISM), and that recurrent fluorescence (RF) may provide a pertinent survival mechanism (e.g. M. H. Stockett et al. 2023; J. E. Navarro Navarrete et al. 2023; F. C. Daly et al. 2023, 2024; T. E. Douglas-Walker et al. 2025; A. Subramani et al. 2026). The crucial context is the important B. A. McGuire et al. (2018, 2021) findings, who discovered an overabundance of neutral cyanonaphthalene and benzonitrile in the dense molecular cloud TMC-1 relative to models (see also M. C. McCarthy & B. A. McGuire 2026). A proposal to be explored that possibly reduces the offset posits smaller aromatic cations were potentially inherited from the diffuse ISM, with the caveat that RF bolstered their survival in that environment (e.g. F. C. Daly et al. 2023, 2024, and broader discussion therein).

Cyanonaphthalene ($C_{10}H_7CN$, CNN) and benzonitrile (C_6H_5CN, BZN) exhibit 11 and 7 carbon atoms, respectively, and the existing consensus regarding the absence of such smaller aromatics was articulated by several studies (e.g. T. Allain, S. Leach & E. Sedlmayr 1996; V. Le Page, T. P. Snow & V. M. Bierbaum 2003; J. Montillaud, C. Joblin & D. Toublanc 2013; A. Omont & H. F. Bettinger 2025). Those smaller aromatics have decreased vibrational modes to diffuse excess energy. M. H. Stockett et al. (2023, fig. 4B) deduced that intramolecular vibrational redistribution (IVR) dictates a comparatively negligible survival probability for $C_{10}H_7CN+$ near $\simeq$ 5.25 eV, and importantly that RF extends the aforementioned threshold to $\simeq$ 7 eV (e.g. $\simeq$ 20 per cent survivability with RF at 5.75 eV). As a result neutral cyanonaphthalene could transform into a stable cation after photoionization by a single 13.6 eV strike (ionization potential is $\simeq$ 8.6 eV; e.g. V. Shivatare, S. Y. Tzeng & W. B. Tzeng 2013). However, as crucially re-emphasized here: in the diffuse ISM such destructive photons striking the resulting cation are unceasing (i.e. the interstellar radiation field, ISRF, Fig. 1), which overturns the long-term survivability argument for that cation in concert with dissociative recombination (Section 2.1). Indeed, that same survival problem exists with the photodissociation region (PDR) or diffuse ISM cases considered for cyanoindene cation (for alternate viewpoints see T. E. Douglas-Walker et al. 2025; A. Subramani et al. 2026). Comparatively hostile PDR regions are discussed by O. Berné & A. G. G. M. Tielens (2012) and J. Montillaud et al. (2013).

Here, the time-scale for dissociative recombination relies partly on the J. P. Wiens, N. S. Shuman & A. A. Viggiano (2015) molecular cross-section to disfavor the existence of $C_{10}H_7CN+$ in the diffuse ISM (equation 1, Section 2.1), and that is paired with an estimate tied to fragmenting photons from diverse ISRFs including C. C. Popescu et al. (2017) (equation 4, Section 2.2). The study aims to quantitatively support certain assertions by D. Majaess et al. (2026) regarding the lack of BZN+ in the diffuse ISM, semi-independently reaffirm existing $N_C \approx 7$–11 non-survivability claims (e.g. J. Montillaud et al. 2013), and ultimately

★ E-mail: Daniel.Majaess@msvu.ca

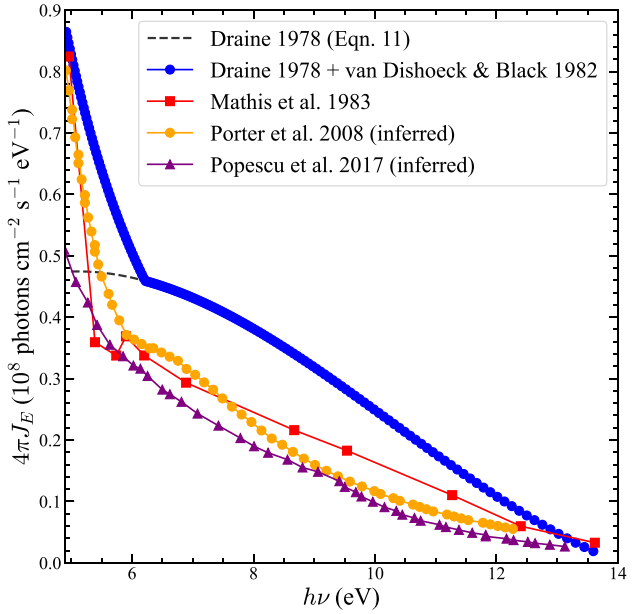

Figure 1. Diverse ISRFs employed to estimate the time-scale of dissociating photons for $C_{10}H_7CN+$, and uncertainty spread. Data are from a combined B. T. Draine (1978) and E. F. van Dishoeck & J. H. Black (1982) set which is the standard ISRF at van Dishoeck's website (see also A. N. Heays, A. D. Bosman & E. F. van Dishoeck 2017), J. S. Mathis, P. G. Mezger & N. Panagia (1983, their table A3), T. A. Porter et al. (2008, inferred from their fig. 1, right panel), and C. C. Popescu et al. (2017, inferred from their fig. 9, bottom left panel).

counter the viability of such smaller aromatics as DIB sources. Admittedly, RF may enhance the survivability of a subsample of aromatics whose structure is amenable to the process; however, that revised carbon number is larger than $C_{10}H_7CN+$. For example, A. Omont & H. F. Bettinger (2025) suggest an RF revised lower bound of $N_C \approx 25$–30 (diffuse ISM).

2 ANALYSIS

2.1 Dissociative recombination time-scale

The recombination time-scale for an electron–cation encounter can be approximated via an Arrhenius-type formula (e.g. equation 1 in D. McElroy et al. 2013):

$$\tau \approx (n_e k)^{-1} \approx \left(n_e \alpha \left(\frac{T}{T_{\rm ref}} \right)^{\beta} \right)^{-1} \quad (1)$$

Where T is the temperature, β modulates the temperature dependence, α is the reaction rate coefficient, k is the effective rate, and n_e is the electron density. J. P. Wiens et al. (2015) deduced that $\alpha = (9 \pm 3) \cdot 10^{-7}$ cm^3 s^{-1} for the naphthalene cation ($T_{\rm ref} = 300$ K), which shall be used as a proxy for cyanonaphthalene cation, and consequently the cited uncertainty range was doubled. A diffuse ISM temperature of $T = [30, 100]$ K stems from T. P. Snow & B. J. McCall (2006) (see also E. L. O. Bakes & A. G. G. M. Tielens 1994). An electron density range of $n_e = [0.01, 0.06]$ cm^{-3} was detailed by S. Harrison, A. Faure & J. Tennyson (2013), and the topic is likewise discussed elsewhere (e.g. B. T. Draine 1978; J. H. Black & E. F. van Dishoeck 1991; J. Montillaud et al. 2013; S. K. Ocker, J. M. Cordes & S. Chatterjee 2020). Parameters employed to discern the time-scale are summarized in Table 1, and the impact of uncertainties are shown in Fig. 2.

The deduced time-scale is $\tau \approx 0.5^{+5.6}_{-0.4}$ yr, and throughout the work the time-scale bounds relay the full range rather than smaller standard deviations. The ionization energy of neutral cyanonaphthalene is $\simeq 8.6$ eV (e.g. V. Shivatare et al. 2013). Therefore, the electron–cation recombination will be dissociative, since the potential energy released upon neutralization exceeds the IVR 5.25 eV limit. That threshold is applicable granted T. Allain et al. (1996) relied partly on S. Leach (1987) to con-

Table 1. Parameters adopted for the time-scale estimates.

Parameter	Value	Source
T	30–100 K	(1)
α	$(9 \pm 3) \cdot 10^{-7}$ cm^3 s^{-1}	(2)
n_e	0.01–0.06 cm^{-3}	(3)
β	−0.5	(4)
σ	$N_c \cdot (7 \cdot 10^{-18}$ cm^2)	(5)
γ	2–3	(6)
A_V	0–1	(7)

Note. references are T. P. Snow & B. J. McCall (2006) (1), J. P. Wiens et al. (2015) (2), S. Harrison et al. (2013) (3), D. McElroy et al. (2013) (4), O. Berné & A. G. G. M. Tielens (2012) with reference to A. G. G. M. Tielens (2005) (5), table 18 data in A. N. Heays et al. (2017) (6), and T. P. Snow & B. J. McCall (2006) (7). The following final values were adopted to address uncertainties (see text): $\alpha = [3 \cdot 10^{-7}, 15 \cdot 10^{-7}]$ cm^3 s^{-1} (naphthalene cation proxy for cyanonaphthalene cation), and $\sigma \approx N_c \cdot [3.5 \cdot 10^{-18}, 10.5 \cdot 10^{-18}]$ cm^2.

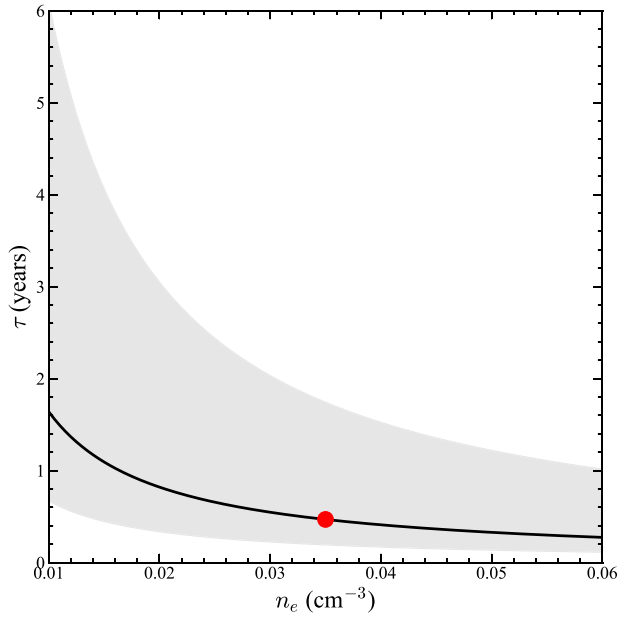

Figure 2. Approximate diffuse ISM time-scale for a dissociative recombination encounter between an electron and $C_{10}H_7CN+$ ($\tau \approx 0.5^{+5.6}_{-0.4}$ yr, Section 2.1). The datum represents nominal values, and the uncertainty bounds relay the full range (i.e. maximum and minimum of equation 1).

clude that for such molecules cation and neutral IVR dynamics are comparable, since the intramolecular dynamics, dissociation energies, and vibrational frequencies are similar. Moreover, the energized neutral PAH initially sits at the equilibrium geometry of the cation. Note the RF mechanism is not viable for the neutral species owing to the missing < 2 eV low-lying states criterion, as V. Shivatare et al. (2013) deduced that the $S_1 \leftarrow S_0$ origin of neutral 1-CNN corresponds to ~ 3.9 eV. The absence of an effective RF channel further shifts the fate of the molecule towards dissociation. Furthermore, V. Le Page, T. P. Snow & V. M. Bierbaum (2001) applied the same Rice–Ramsperger–Kassel–Marcus (RRKM) statistical framework used for photodissociation to the recombination branching ratio, and found that recombination becomes nondissociative for pyrene cations and larger ($N_c \geq 16$), implying destruction of the smaller $C_{10}H_7CN+$. In sum, the evidence favours a destructive outcome.

The time-scale for the smaller benzonitrile cation is ≈ 3 yr given $\alpha \approx 1.5 \cdot 10^{-7}$ cm^3 s^{-1} (benzene cation proxy, UMIST,[1] see also D. McElroy et al. 2013). D. Majaess et al. (2026) identified that a holistic evidentiary framework suggests that benzonitrile cation is relatively absent in the diffuse ISM: e.g. RF being an improbable mechanism in this case, mismatches between diffuse interstellar bands (DIBs) and advantageous F. C. Daly et al. (2024) experimental results (bypassed existing sizable matrix effects), and the hitherto absence of DIBs matching any similarly sized cations. That latter point, concurrent with the assertions raised here, likewise applies to the other molecules discussed.

2.2 Photodissociation time-scale

Neutral cyanonaphthalene can survive 13.6 eV photoionization and the excess is redistributed via the cation's IVR, with RF providing the radiative stabilization channel. However, as noted the concern is not with an isolated strike, but unceasing dissociating photons (Figs 1, 3).

To estimate the time-scale for dissociating 7–13.6 eV photons the following ISRFs were investigated: a combined B. T. Draine (1978) and E. F. van Dishoeck & J. H. Black (1982) data set that is the standard ISRF at van Dishoeck's website[2] (see also A. N. Heays et al. 2017; J. S. Mathis et al. 1983; T. A. Porter et al. 2008; C. C. Popescu et al. 2017). Fig. 1 conveys the ISRFs, and for example, references that B. T. Draine (1978) relied on are conveyed in their fig. 3 caption. Data from ISRF diagrams in T. A. Porter et al. (2008) and C. C. Popescu et al. (2017) were extracted using PLOTDIGITIZER.

The photodestructive time-scale can be approximated as (e.g. equation 1 in A. N. Heays et al. 2017):

$$\tau = k^{-1} = \left[\int_{E_1}^{E_2} \sigma(E) \cdot 4\pi J_E \, dE \right]^{-1} \quad (2)$$

Where k is the rate constant, $\sigma(E)$ is the molecular cross-section, and $4\pi J_E$ is the flux (photons cm^{-2} s^{-1} eV^{-1}). The molecular cross-section can be recast in terms of carbon number (O. Berné & A. G. G. M. Tielens 2012, who reference A. G. G. M. Tielens 2005):

$$\sigma(E) \approx \sigma \approx N_C \cdot (7 \cdot 10^{-18} \text{ cm}^2) \quad (3)$$

The coefficient was adjusted to sample an uncertainty breadth of 50 per cent (i.e. $\sigma \approx N_C \cdot [3.5 \cdot 10^{-18}, 10.5 \cdot 10^{-18}]$ cm^2). Inserting the approximation into equation (2) yields:

$$\tau \approx \left[4\pi N_C (7.0 \pm 3.5) \cdot 10^{-18} \text{cm}^2 \int J_E \, dE \right]^{-1} \quad (4)$$

The function was evaluated using numerical integration (trapezoid), where the ISRFs were each interpolated at 0.01 eV steps (grid). The resulting time-scale for 7–13.6 eV dissociating photons is $\tau \approx 4^{+7}_{-2}$ yr ($A_V = 0$, cyanonaphthalene cation). The bounds include values spanned by the diverse ISRFs. An additional datum was added to the inferred T. A. Porter et al. (2008) and C. C. Popescu et al. (2017) findings near 13.6 eV, which is an average of B. T. Draine (1978) and J. S. Mathis et al. (1983).

Alternatively, to approximate a time-scale one can proceed directly with the equation (11) polynomial from B. T. Draine (1978), as described below. A caveat is highlighted in Fig. 1 regarding the relation's comparative underestimation near $\simeq 5$ eV, and relative overestimation towards shorter wavelengths. B. T. Draine (1978) indicates their polynomial is solely for the $\simeq$ 5–13.6 eV range.

$$\tau \approx \left[\zeta \int \left(1.658 \cdot 10^6 E - 2.152 \cdot 10^5 E^2 + 6.919 \cdot 10^3 E^3 \right) dE \right]^{-1}$$
$$\approx \left[\zeta \left(8.290 \cdot 10^5 E^2 - 7.173 \cdot 10^4 E^3 + 1.730 \cdot 10^3 E^4 \right) \Big|_{E_0}^{E_f} \right]^{-1} \quad (5)$$

Where $\zeta = 4\pi\sigma$ was implemented to fit the equation within the allowed column width. For 7–13.6 eV photons $\tau \approx 3$ yr (cyanonaphthalene cation), while for benzonitrile $\tau \approx 4$ yr ($A_V \approx 0$). The results are consistent with those inferred from the equation described in section 4.1 of A. G. G. M. Tielens (2026).

Accounting for total visible dust extinction ($A_V = 0$–1) increases τ by an order of magnitude. Applying a dust attenuation approximation that is equation (14) in A. N. Heays et al. (2017) to

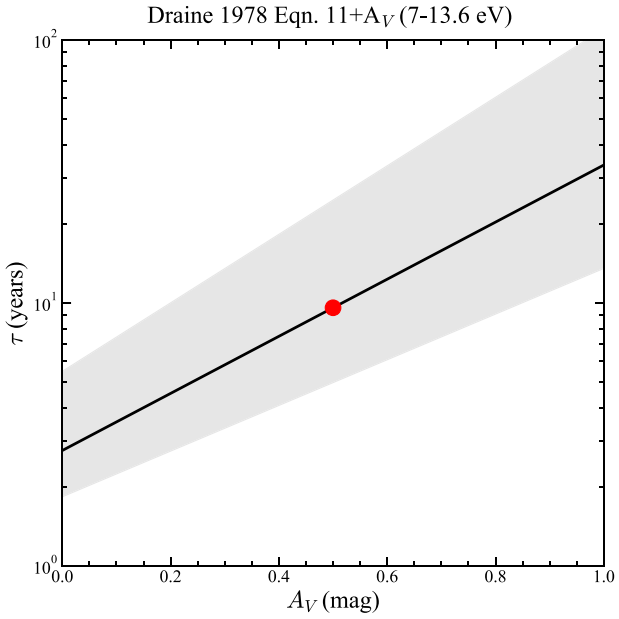

Figure 3. Equation (11) ISRF in B. T. Draine (1978) plus an extinction term provides an alternate photodestructive time-scale ($\tau \approx 10^{+101}_{-8}$ yr for $C_{10}H_7CN+$, assuming $A_V = 0$–1, equation 7). Smaller aromatics are struck incessantly by 7–13.6 eV photons in the diffuse ISM, which is paired with unrelenting dissociative recombination (Section 2.1).

[1] https://umistdatabase.uk
[2] https://home.strw.leidenuniv.nl/~ewine/photo/radiation_fields.html

equation (4):

$$\tau \approx e^{\gamma A_V}\tau_0 \approx e^{\gamma A_V}\left[4\pi N_c(7.0\pm3.5)\cdot10^{-18}\mathrm{cm}^2\int J_E\,dE\right]^{-1} \quad (6)$$

Where $\gamma \approx 2$–3 is the dust shielding parameter, and the range stems from near the median and standard deviation of Table 18 data in A. N. Heays et al. (2017). The time-scale expands to $\tau \approx 16^{+223}_{-14}$ yr. The uncertainty range displayed represents end to end bounds. The time-scale nearly halves to 9 yr when adopting the $\simeq 5.25$ eV bound (no RF, fig. 4B in M. H. Stockett et al. 2023).

Recasting equation (11) in B. T. Draine (1978) to include the extinction approximation:

$$\tau \approx \frac{e^{\gamma A_V}}{\left[\zeta\left(8.290\cdot10^5E^2-7.173\cdot10^4E^3+1.730\cdot10^3E^4\right)\Big|_{E_0}^{E_f}\right]} \quad (7)$$

The ensuing time-scale for $C_{10}H_7CN$ + photodestruction is $\tau \approx 10^{+101}_{-8}$ yr (Fig. 3).

Both nominal dissociative recombination and photodestruction time-scales could be uncertain by an order of magnitude. Yet a diffuse ISM bottom-up carbon interaction is possibly orders of magnitude longer (T. Allain et al. 1996, see also fig. 1 of A. Omont & H. F. Bettinger 2021). Conversely, within the uncertainties, hydrogenation can occur on time-scales of comparable order to the aforementioned electrons and photons; however, A. Omont & H. F. Bettinger (2021) ultimately favour small PAH skeletal destruction in the diffuse ISM (see also A. Omont & H. F. Bettinger 2025).

3 CONCLUSIONS

Experimental characterizations of RF were seminal (M. H. Stockett et al. 2023). However, that mechanism may not overturn existing models advocating for the absence of $N_C \approx 7$–11 diffuse ISM aromatics (e.g. $C_{10}H_7CN$+). That conclusion partly relies on an approximated dissociative recombination time-scale tied to the J. P. Wiens et al. (2015) molecular cross-section ($\tau \approx 0.5^{+5.6}_{-0.4}$ yr), and photodestruction time-scale linked to diverse ISRFs ($\tau \approx 16^{+223}_{-14}$ yr for $A_V = 0$–1, or $\tau \approx 4^{+7}_{-2}$ yr at $A_V \approx 0$). Neutral cyanonaphthalene may sustain photoionization, but the ensuing cation will not survive unceasing photon and dissociative recombination encounters. Consequently, inheritance of comparably sized cations from the diffuse ISM may not partially explain observed overabundances of neutral cyanonaphthalene or benzonitrile in dense TMC-1 (see also J. Cernicharo et al. 2023, who arrived at part of this conclusion for benzonitrile from a separate vantage point).

As a result DIBs are improbably tied to cations of cyanonaphthalene, benzonitrile, or cyanoindene (see also D. Majaess et al. 2026, and for broader context fig. 15 in A. G. G. M. Tielens 2026). Regarding the C≡N vibrational signature identified by D. Majaess et al. (2025) in a histogram of energy differences between highly correlated DIB pairs, it follows that diffuse ISM feature is unrelated to cyanonaphthalene or benzonitrile cations (i.e. unassociated with smaller aromatics). Specifically, D. Majaess et al. (2025) conveyed that a histogram sampling the entire APO catalogue (H. Fan et al. 2019) could broadly reveal bonds endemic to DIB sources (e.g. aromatics, oop C−H bending); however, that initial framework requires (in)validation. Energy differences between interrelated DIBs sharing a common carrier may reveal vibrational transitions (e.g. P. Jenniskens & F. X. Desert 1993; A. Bondar 2020). The C≡N detection may consequently be tied to larger PAHs, MAONs (S. Kwok 2022), or perhaps integrated in a fullerene structure (A. Omont 2016). The important acquisition of molecular spectra for aromatic nitriles continues unabated (e.g. F. C. Daly et al. 2023; T. E. Douglas-Walker et al. 2025).

ACKNOWLEDGEMENTS

This research relied on initiatives such as NASA ADS, arXiv, UMIST, ISRFs of fellow researchers, and the Apache Point Observatory DIB catalogue. Access to PYTHON tools was facilitated by vibcoding in Gemini 3.

DATA AVAILABILITY

The data underlying this article are readily available in the literature or sources cited.

REFERENCES

Allain T., Leach S., Sedlmayr E., 1996, A&A, 305, 602
Bakes E. L. O., Tielens A. G. G. M., 1994, ApJ, 427, 822,
Berné O., Tielens A. G. G. M., 2012, Proc. Natl. Acad. Sci., 109, 401
Black J. H., van Dishoeck E. F., 1991, ApJ, 369, L9
Bondar A., 2020, MNRAS, 496, 2231
Cernicharo J., Tercero B., Marcelino N., Agúndez M., de Vicente P., 2023, A&A, 674, L4
Daly F. C., Palotás J., Jacovella U., Campbell E. K., 2023, A&A, 677, A128
Daly F. C., Douglas-Walker T. E., Palotás J., Anstöter C. S., Zheng A., Campbell E. K., 2024, J. Chem. Phys., 161, 074305
Douglas-Walker T. E. et al., 2025, ACS Earth Space Chem., 9, 134
Draine B. T., 1978, ApJS, 36, 595
Fan H. et al., 2019, ApJ, 878, 151
Harrison S., Faure A., Tennyson J., 2013, MNRAS, 435, 3541
Heays A. N., Bosman A. D., van Dishoeck E. F., 2017, A&A, 602, A105
Jenniskens P., Desert F. X., 1993, A&A, 274, 465
Kwok S., 2022, Ap&SS, 367, 16
Le Page V., Snow T. P., Bierbaum V. M., 2001, ApJS, 132, 233
Le Page V., Snow T. P., Bierbaum V. M., 2003, ApJ, 584, 316
Leach S., 1987, in Leger A., D'Hendecourt L., Boccara N., eds, NATO Advanced Study Institute (ASI) Series C Vol. 191, Polycyclic Aromatic Hydrocarbons and Astrophysics. Reidel, Dordrecht, p. 99
Majaess D., Seuret H., Harriott T. A., Morera-Boado C., Sullivan A. D., Massa L., Matta C. F., 2025, MNRAS, 539, 3489
Majaess D., Morera-Boado C., Harriott T. A., Rahi Q., Seuret H., Massa L., Matta C. F., 2026, preprint (arXiv:2603.23739)
Mathis J. S., Mezger P. G., Panagia N., 1983, A&A, 128, 212
McCarthy M. C., McGuire B. A., 2026, Annu. Rev. Phys. Chem., 77, 345
McElroy D., Walsh C., Markwick A. J., Cordiner M. A., Smith K., Millar T. J., 2013, A&A, 550, A36
McGuire B. A., Burkhardt A. M., Kalenskii S., Shingledecker C. N., Remijan A. J., Herbst E., McCarthy M. C., 2018, Science, 359, 202
McGuire B. A. et al., 2021, Science, 371, 1265
Montillaud J., Joblin C., Toublanc D., 2013, A&A, 552, A15
Navarro Navarrete J. E. et al., 2023, Faraday Discuss., 245, 352
Ocker S. K., Cordes J. M., Chatterjee S., 2020, ApJ, 897, 124
Omont A., 2016, A&A, 590, A52
Omont A., Bettinger H. F., 2021, A&A, 650, A193
Omont A., Bettinger H. F., 2025, A&A, 696, A180
Popescu C. C., Yang R., Tuffs R. J., Natale G., Rushton M., Aharonian F., 2017, MNRAS, 470, 2539

Porter T. A., Moskalenko I. V., Strong A. W., Orlando E., Bouchet L., 2008, ApJ, 682, 400
Shivatare V., Tzeng S. Y., Tzeng W. B., 2013, Chem. Phys. Lett., 558, 20
Snow T. P., McCall B. J., 2006, ARA&A, 44, 367
Stockett M. H. et al., 2023, Nat. Commun., 14, 395
Subramani A. et al., 2026, ApJ, 997, 49
Tielens A. G. G. M., 2005, The Physics and Chemistry of the Interstellar Medium. Cambridge Univ. Press, Cambridge, UK
Tielens A. G. G. M., 2026, ACS Earth Space Chem., 10, 942
van Dishoeck E. F., Black J. H., 1982, ApJ, 258, 533
Wiens J. P., Shuman N. S., Viggiano A. A., 2015, J. Chem. Phys., 142, 114304

This paper has been typeset from a TEX/LATEX file prepared by the author.